Volume 25
Number 8
August 2023
Pages 1255–1420

# Environmental Science
## Processes & Impacts

rsc.li/espi

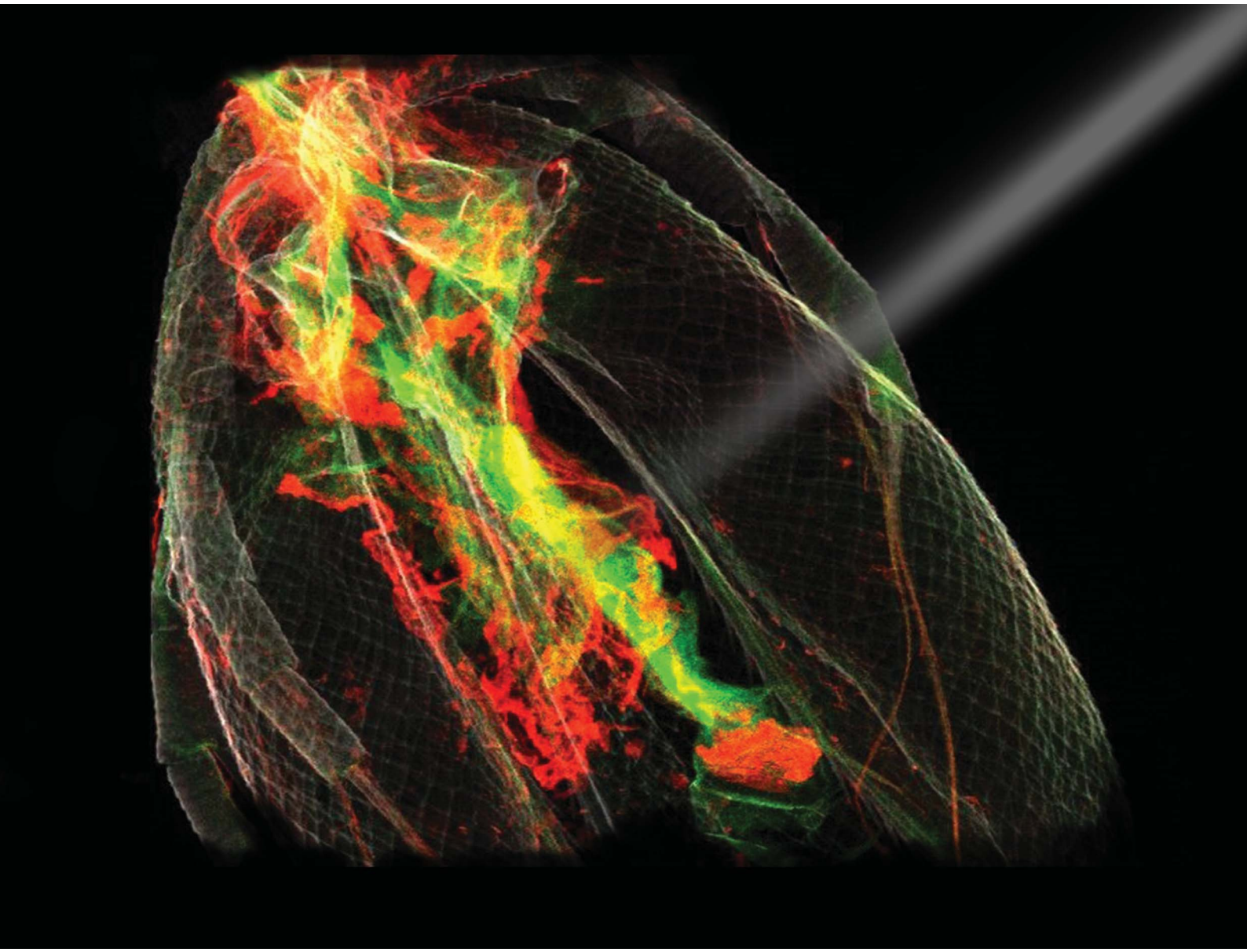

ISSN 2050-7887

ROYAL SOCIETY OF CHEMISTRY

**PAPER**
Marion Revel *et al.*
Determination of the distribution of rare earth elements La and Gd in *Daphnia magna via* micro and nano-SXRF imaging

View Article Online

Environmental Science Processes & Impacts

ROYAL SOCIETY OF CHEMISTRY

PAPER



Cite this: *Environ. Sci.: Processes Impacts*, 2023, **25**, 1288

# Determination of the distribution of rare earth elements La and Gd in *Daphnia magna via* micro and nano-SXRF imaging†

Marion Revel, *[ab] Kadda Medjoubi,[c] Camille Rivard,[cd] Delphine Vantelon, [c] Andrew Hursthouse [b] and Susanne Heise[a]

While our awareness of the toxicity of rare earth elements to aquatic organisms increases, our understanding of their direct interaction and accumulation remains limited. This study describes the acute toxicity of lanthanum (La) and gadolinium (Gd) in *Daphnia magna* neonates and discusses potential modes of action on the basis of the respective patterns of biodistribution. Ecotoxicological bioassays for acute toxicity were conducted and dissolved metal concentrations at the end of the tests were determined. The results showed a significant difference in nominal $EC_{50}$ (immobility) between La (>30 mg $L^{-1}$) and Gd (13.93 (10.92 to 17.38) mg $L^{-1}$). Daphnids that were then exposed to a concentration close to the determined $EC_{50}$ of Gd (15 mg $L^{-1}$, nominal concentration) for 48 h and 72 h were studied by synchrotron micro and nano-X-ray fluorescence to evaluate the biodistribution of potentially accumulated metals. X-ray fluorescence analyses showed that La was mainly found in the intestinal track and appeared to accumulate in the hindgut. This accumulation might be explained by the ingestion of solid La precipitates formed in the media. In contrast, Gd could only be detected in a small amount, if at all, in the intestinal tract, but was present at a much higher concentration in the tissues and became more pronounced with longer exposure time. The solubility of Gd is higher in the media used, leading to higher dissolved concentrations and uptake into tissue in ionic form *via* common metal transporting proteins. By studying La and Gd biodistribution in *D. magna* after an acute exposure, the present study has demonstrated that different uptake pathways of solid and dissolved metal species may lead to different accumulation patterns and toxicity.

Received 7th April 2023
Accepted 24th May 2023

DOI: 10.1039/d3em00133d

rsc.li/espi



### Environmental significance

The increasing use of rare earth elements (REEs) in modern technologies has raised concerns about their potential environmental impact, making it urgent to better understand their potential effect on aquatic organisms. The application of synchrotron nano and micro XRF techniques provided valuable insights into the biodistribution of lanthanum (La) and gadolinium (Gd), and revealed the differential behavior and toxicity of these metals on *D. magna*, which seems to be attributed to their speciation. The results highlight the importance of considering metal speciation in REE ecotoxicology and provides a significant baseline on the toxicokinetics of Ln in the environment. Therefore, the present paper contributes to the advancement of knowledge on the mode of action of REEs and underscores the necessity for continued research on the toxicity and fate of REEs.

## 1. Introduction

Rare earth elements are a group of 16 elements containing the 15 lanthanides (Ln) and yttrium (Y). With an ever increasing demand for Ln in modern technologies, these metals are now considered to be emerging pollutants.[1] Little is known about the effects of the Ln on aquatic organisms. Aquatic invertebrates such as water fleas seem to be particularly sensitive to Ln.[2] As they have a key role in the aquatic food web, it is of great importance to understand how and to what extent they are affected by elevated Ln concentrations in their environment. Studies on daphnids suggest that lanthanum toxicity could be comparable to that of copper (Cu).[3,4] Acute toxicity on *Daphnia magna* ($EC_{50}$ of thorium (Th) and cerium (Ce) = 1.09 and 2.48 mg $L^{-1}$, respectively) appears to be dependent on the chemical form of the metal.[5] Chronic exposure to Ce, erbium (Er) or Th at concentrations higher than 0.43 μg $L^{-1}$ impacted on reproduction, growth and survival of *D. magna*.[5,6] Due to similar ionic radii of $Ln^{3+}$ and calcium ($Ca^{2+}$) ions they might

[a]*Life Sciences, Hamburg University of Applied Science, Ulmenliet 20, D-21033 Hamburg, Germany. E-mail: marion.revel@haw-hamburg.de*
[b]*University of the CWest of Scotland, Paisley, PA1 2BE, UK*
[c]*SOLEIL synchrotron, L'Orme des Merisiers, Dptale 128, 91190 Saint-Aubin, France*
[d]*TRANSFORM, INRAE, 44316 Nantes, France*

† Electronic supplementary information (ESI) available. See DOI: https://doi.org/10.1039/d3em00133d

compete for binding sites on cell membranes.[4] The trivalent Ln ions have been shown to block Ca channels and disturb enzyme activities.[7]

However, despite their similar properties, lanthanides have been shown to vary in their toxicity to aquatic organisms.[8–10] By assessing the toxicity of one light and one medium/heavy REE; lanthanum (La) and gadolinium (Gd) salts to *D. magna* and comparing this with the resulting elemental biodistribution, we tried to elucidate, whether any difference in toxicity could be due to a difference of toxikokinetics (uptake, distribution, accumulation).

Toxikokinetc studies of REE are rare and observations of biodistribution have so far mostly been performed on either nanoparticles or Gd contrast agents (GdCA). Synchrotron micro X-ray fluorescence spectroscopy showed for example for $LaCoO_3$ perovskite nanoparticles that aggregates were taken up with food and found in the gut of *D. magna*.[11] With increasing $LaCoO_3$ concentration, the dissolved La accumulated in the thoracic limbs.[11] Oxidative stress was induced regardless the nominal concentration, and the highest dose altered the $Na^+$/$K^+$-ATPase activity. With Gd based contrast agents (GdCA), accumulation in *D. magna* was studied by laser ablation inductively coupled plasma mass spectrometry.[12] Gd was found in the intestine and carapace of the daphnids after 19 h of exposure but no further information on the toxicity of Gd-CA was provided. The exposure to Ln salts, discussed here reveals different biodistribution patterns and provides insight to the impact of dissolved Ln exposure. So far, Ln biodistribution in aquatic organisms has only been studied using contrast agents and nanoparticles, and suffered from the difficulty in determining low and potentially diffuse concentrations in organisms. Synchrotron micro and nano X-ray fluorescence offers high spatial resolution 2D mapping and is capable of detecting very low, localized metal concentrations within the organism.[13–16] In our study, elemental biodistribution was characterised in two synchrotron beamlines, permitting a high sensitivity detection for light and heavy elements at different resolutions.

## 2. Materials and methods

### 2.1. *Daphnia magna* culture

*D. magna* adults were purchased from the German Environmental Ministry (Umweltbundesamt) and maintained at the University of Applied Sciences of Hamburg (HAW). The organisms were cultured at 21 ± 1 °C with a 16 : 8 light–dark cycle in Elendt M4 media[17] and fed every day with freshwater algae (*Chlorella vulgaris*).

### 2.2. Acute immobilization test

Tests were performed according to guideline OECD 202 (*Daphnia* sp. acute immobilization test).[18] Test media were prepared according to DIN EN ISO 6341:2013-01 (ref. 19) but sodium (Na) was added as sodium chloride (NaCl) instead of sodium bicarbonate ($NaHCO_3$) in order to limit Ln-carbonate precipitation, pH was maintained at 7.00 ± 0.2, oxygen concentration was higher than 3 mg $L^{-1}$, and salinity did not exceed 0.585 ppt (ESI data S1†).

Neonates of less than 24 h of age were exposed in 6 well plastic plates (VWR International, Radnor, US). For each conditions (La exposure, Gd exposure and controls), 15 organisms were distributed in three wells and 10 mL of medium were added per well. For determination of the $EC_{50}$ of La and Gd, immobilization was studied after 48 h of exposure at different nominal concentrations from 5 to 30 mg Ln $L^{-1}$ added as pure standard solution for ICP-MS of Gd(III) and La(III), (N9300127 and N9300118 for La and Gd respectively, PerkinElmer, Waltham, US). The immobilization of the daphnids refers to the absence of any movement for a period of 15 seconds following a gentle agitation of the test vessel. For statistical analysis, a minimum of four repetitions of this experimental setup were performed. $EC_{50}$ values were determined by nonlinear regression using GraphPad Prism version 8.0.

### 2.3. Chemical analysis and speciation modelling

The dissolved Ln concentration in the test media was measured after the bioassays. Samples were filtered through 0.2 μm cellulose nitrate filter (Whatman, Maidstone, UK), acidified with $HNO_3$ (Roth, Karlsruhe, Germany) to a final acid concentration of 2% and measured by total reflection X-ray fluorescence spectrometry (TRXF) with a Picofox S2 (Bruker AXS Microanalysis GmbH, Billerica, US). The limit of detection La and Gd in liquid samples was 0.1 mg $L^{-1}$ when measured for 1000 s with 10 mg $L^{-1}$ of Ga as internal standard. This is in line with the limit of detection measured by Telgmann *et al.*[20] for Gd in blood urine (LOD: 0.1 mg $L^{-1}$). Speciation modelling was performed with Visual MINTEQ version 3.1 in order to predict the dissolved and solid forms of La and Gd after equilibrium (ESI data S2†).

### 2.4. Micro and nano-XRF analysis

To spatially investigate the progress of La and Gd accumulation in daphnids, neonates of less than 24 h of age were exposed to 15 mg $L^{-1}$ of La and Gd, respectively, for 48 and 72 h, following the same protocol as described above. At the end of the exposure, the surviving organisms were dehydrated in an increasing acetone–water series (70; 80; 90; 98; 100% of acetone, ten minutes in each) and dried in HDMS (1,1,1,3,3,3-hexamethyldisilazane, MERCK, Darmstadt, Germany) for 30 min according to Laforsch and Tollrian.[21] The samples were then transferred to a desiccator and kept under vacuum overnight.

The spatial distribution of La and Gd was determined using two beamlines of the SOLEIL synchrotron facility (Saint-Aubin, France): NANOSCOPIUM hard X-ray scanning nanoprobe beamline[22] and LUCIA soft X-ray scanning microprobe beamline.[23,24] On NANOSCOPIUM, the incident monochromatic X-ray beam of 17.02 keV energy was focused on the sample position by Kirkpatrick–Baez (KB) mirrors to create a high intensity nano-beam. Profiting from the flexible optical design of NANOSCOPIUM the spatial resolution was adapted to the needs of the experiment by tuning it to few hundred nanometers. The XRF signal was collected with two Si-drift detectors mounted in

the horizontal plane of the beam in backscattering geometry. Full XRF spectra were collected in each pixel and processed by an in-house Matlab code, available at NANOSCOPIUM, to provide a high resolution distribution of multiple elements such as Ca, zinc (Zn), La, and Gd as well as the Compton (inelastic) scattering which permitted to give further organism's detailed internal morphology.[25]

Three organisms per Ln were glued on the pin of a toothpick and were continuously scanned using the FlyScan continuous acquisition mode[26] with 20 to 100 ms of dwell time per pixel with a pixel size of 400 × 400 nm to 1 × 1 μm, depending on the field of view. The correlative RGB maps were analysed using FIJI.[27] The fluorescence intensity of each pixel of La and Gd maps was normalized by the incident intensity of the beam at the respective time of the measurement. The normalized intensity was calculated by multiplying the amount of pixel with the average intensity of Ln. For further information on La distribution in the intestinal tract, a segmented line with a width of 90 μm was traced on FIJI, going from the mouth to the hindgut. A similar line was performed in order to study the metal distribution along the dorso-ventral line of each organism.

To determine the spatial distribution with a better signal to noise ratio of light elements such as sulphur (S) and phosphorus (P), the samples were analysed on LUCIA beamline. Daphnids (6 Ln contamined and 8 controls) were mounted between two layers of Ultralene (SPEX SamplePrep, Metuchen, US; 4 μm thick) in copper sample holders and analyses were conducted under vacuum.

The monochromatic X-ray beam of 7.25 keV energy was focused to 3.2 × 2.6 ($h \times v$) $\mu m^2$ by means of a KB mirrors arrangement. The XRF signal was collected using a 60 $mm^2$ silicon drift diode Bruker detector. The pixel size was 3 × 3 $\mu m^2$ with an integration time of 50 to 80 ms per pixel.

The XRF signal of each detected element was extracted by batch fitting the XRF spectrum recorded in each pixel of the maps using PyMCA software.[28] The count number of the XRF signal was corrected by the XRF detector deadtime values in each pixel. Correlative RGB maps were plotted using Fiji. To extract quantitative data, the average XRF spectra of each daphnids was extracted by selecting all the pixels corresponding to daphnids using PyMCA selection tool based on pixel intensity. The average XRF spectra were then fitted to obtain the Ca and Ln peak areas values and thus calculate the Ca/Ln ratio for each daphnid.

# 3. Results

## 3.1. Ecotoxicological assays

Concentrations of La and Gd in the media and the respective daphnid immobilization rate after 48 h of exposure are presented in Table 1. After 48 h of exposure, dissolved La concentrations were significantly lower than the initial concentrations (called nominal concentrations). All concentrations were between 2 and 3 mg $L^{-1}$ except for samples at the nominal concentration of 30 mg $L^{-1}$ where the measured concentration was even lower (0.46 ± 0.01 mg $L^{-1}$). The dissolved concentration slightly increased from 5 to 10 mg $L^{-1}$ and decreased from 10 to 30 mg $L^{-1}$. No inhibition of mobility was measured on the daphnid regardless the concentration.

In the case of Gd, a lower discrepancy between nominal and dissolved concentration after exposure was noted. At 5 mg $L^{-1}$, the dissolved concentration measured was 2.91 ± 0.22 mg $L^{-1}$. This concentration increased until a nominal concentration of 20 mg $L^{-1}$ (9.21 ± 1.95 mg $L^{-1}$). The immobilization rate increased with increasing nominal Gd concentration, from 0% in the control condition to 80.74 ± 13.51%. Further analysis of the dissolved Ln concentration in solution prior to commencing the experiments confirmed the presence of a soluble Ln form. Specifically, at the nominal concentration of 15 mg $L^{-1}$, the dissolved Gd concentration was 15.07 mg $L^{-1}$ and La concentration was 11.87 mg $L^{-1}$, representing 79 to 100% of the nominal concentration. Therefore, metal precipitation is expected to occur during the bioassay.

No immobilization was measured above 8.34% during the bioassays using La (Fig. 1). Therefore, the calculation of $EC_{50}$ was not possible. In contrast, the immobilization rate of *D. magna* decreased with the increase of nominal Gd concentrations and the nominal $EC_{50}$ was calculated at 13.93 mg $L^{-1}$. However, toxicity values based on the measured metal concentration is considered to be more realistic and is recommended.[4,18] Again, only Gd measured $EC_{50}$ was calculated and was at 8.22 mg $L^{-1}$.

## 3.2. Ln distribution in the organisms

Fig. 2 presents correlative distribution of several nano-SXRF elemental maps. To outline the structure of the organisms, the distribution of Ca is presented in grey and the respective lanthanides in red. Fig. 2a depicts biodistribution in a neonate exposed to 15 mg $L^{-1}$ of La for 48 h. La is prominently located in the intestinal tract, until the post abdominal claw. The highest intensity was detected in the middle of the intestinal tract. Lower intensity is found in the thorax of the animal. The distribution of La in neonates exposed for 72 h is presented in Fig. 2b and c. The two maps show similar distribution as shown in Fig. 2a, with La concentrated at the end of the intestinal tract and in some internal structures in the thorax. The maps in Fig. 2c show an internal structure organized in cluster which presents a very similar distribution of La, S, Zn and iron (Fe) in an internal structure located in the top of the abdomen of the daphnid (ESI data S3†).

Fig. 2d and e depicts the Gd distribution of two organisms exposed to 15 mg $L^{-1}$ of Gd for 48 h. In contrast to La accumulation, Gd is visible in a diffuse form in the inside of the organism, in several organs such as the respiratory organs, the intestine or the shell gland (ESI data S4†). Gd accumulation is also visible on the anthenna extremities, the articulations and on the carapace. After 72 h of exposure, Gd highly accumulated in the area of the antenna articulation and at the base of the apical spine.

The organism's detailed internal morphology can be visualised by Compton (inelastic) scattering.[25] The resulting Compton scatter map of the daphnids performed at NANOSCOPIUM

 

Table 1 La and Gd concentration (mg $L^{-1}$) measured by total reflection X-ray fluorescence and mobility rate (%) of *D. magna* exposed for 48 h at nominal concentrations from 5 to 30 mg $L^{-1}$. ±: standard deviation and *n*: number of replicates

| La or Gd nominal concentration (mg $L^{-1}$) | | 5 | 10 | 15 | 20 | 25 | 30 |
|---|---|---|---|---|---|---|---|
| La | Measured dissolved concentration after exposure (mg $L^{-1}$) | 2.55 ± 0.13 | 2.91 ± 3.30 | 2.08 ± 0.83 | 2.00 ± 1.59 | 1.94 ± 1.66 | 0.46 ± 0.01 |
| | Immobilization rate (%) | 0.00 ± 0.00 | 1.67 ± 2.89 | 5.00 ± 8.66 | 1.33 ± 2.67 | 0.00 ± 0.00 | 8.34 ± 10.93 |
| | *n* | 4 | 4 | 4 | 5 | 4 | 4 |
| Gd | Measured dissolved concentration after exposure (mg $L^{-1}$) | 2.91 ± 0.22 | 6.82 ± 1.27 | 7.92 ± 1.82 | 9.21 ± 1.95 | 8.39 ± 2.15 | 9.54 ± 1.50 |
| | Immobilization rate (%) | 3.81 ± 5.25 | 30.67 ± 12.65 | 49.52 ± 15.33 | 43.34 ± 15.94 | 64.77 ± 12.60 | 80.74 ± 13.51 |
| | *n* | 7 | 10 | 7 | 8 | 7 | 9 |

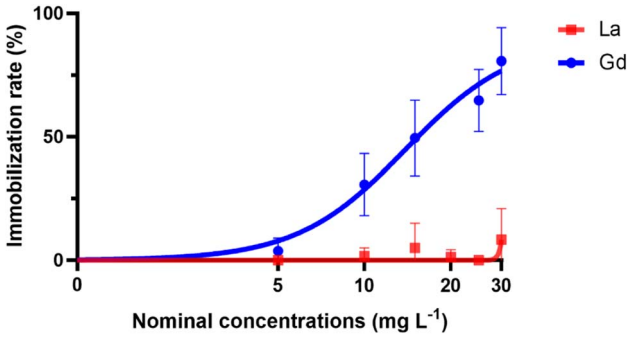


Fig. 1 Nonlinear regression curves of the immobilization rate (%) *versus* nominal concentrations of La and Gd.

beamline, clearly outlined the intestine within the specimens (ESI data S5†).

### 3.3. Ln distribution in the organisms

The normalized intensity of La measured in the organisms and in their intestinal tract is presented in Fig. 3 (Table available in ESI data S6†). Total La intensity in the whole organism and in their intestinal tract appeared to be approximately the same after 48 and 72 hours of exposure. In contrast, Gd intensity in the observed organisms varied by a factor of almost 6 between those that had been exposed for 48 h on one side (290 and 233; Fig. 2d and e) and for 72 h on the other side (1379.08; Fig. 2f).

LUCIA beamline provided access to lower emission energies and permitted to obtain more accurate light element distribution for S and P maps of specimens at a 7.25 keV (Fig. 4). As major components of proteins (S) and nucleotides (P), these two elements can be expected to be present in all tissues of the organisms. The distribution provided visualisation of the main respiratory organs (the limbs) which were not visible mapping at higher energy, *i.e.* 17.02 keV. Controls were also mapped at 7.25 keV to ensure the absence of Ln in the specimens that were not in contact with Ln during the exposure time. The accumulation of Ln in the different organisms was studied by calculating the ratio between Ln and Ca intensity in the entire specimens mapped on LUCIA (Fig. 5). As was observed at NANOSCOPIUM, La and Gd accumulated differently in the organisms. La was found in the intestinal tract while Gd was more diffused in the tissues (ESI data S7†). The comparison of the Ln/Ca ratio between the different samples permitted to show that the degree of accumulation in the exposed organisms (3 to 4 order of magnitude of difference to the control).

### 3.4. Correlation of Ln distribution with organs and tissues of daphnids

A profile of the intestinal tract line was plotted to visualize the variation of the normalized intensity for La over the intestinal tract (Fig. 6). For all three analyses, most of La was concentrated towards the end of the midgut to the hindgut.

The normalized intensity distribution of La and Gd was studied along the dorso-ventral line of each organism. This distribution strongly varied between La and Gd. Fig. 7 presents the La and Gd normalized intensity along the dorso ventral line of the six daphnids mapped in Fig. 2, exposed for 48 and 72 h. Most of La is detected at a similar location (around 400 μm). For Gd, the distribution is more spread out along the line. The organism exposed to Gd for 72 h showed a higher Gd intensity than for organisms exposed to Gd for 48 h, more distributed along all the dorso-ventral line than for the organisms exposed for 48 h.

## 4. Discussion

Results of Ln exposure to aquatic organisms are inconclusive with respect to the relative toxicities of the metals. While Tai *et al.*[29] found similar toxicities for Ln on marine microalgae, other studies had measured different level of toxicity on freshwater organisms[30] and suggested that their toxicity might be correlated to their atomic number.[31] Also, in the present study, a significant difference in acute toxicity of the applied Ln was measured, with a significantly stronger effect for Gd on daphnid immobilization than for La (Table 2). This finding coincides with the study of Blinova *et al.*[8] who calculated a nominal $EC_{50}$ of 18.5 (17.6–19.4) mg $L^{-1}$ for Gd and 31.1 (22.0–40.2) mg $L^{-1}$ for La.

Bioaccumulation is often considered an indicator of the bioavailable contaminant fraction potentially responsible for toxic effects.[32] However, concentrations measured in whole organisms do not necessarily mean that contaminant–receptor interactions are occurring, and further information is needed on the site of accumulation and whether the contaminants are undergoing active metabolism and affecting the physiology of the animal.

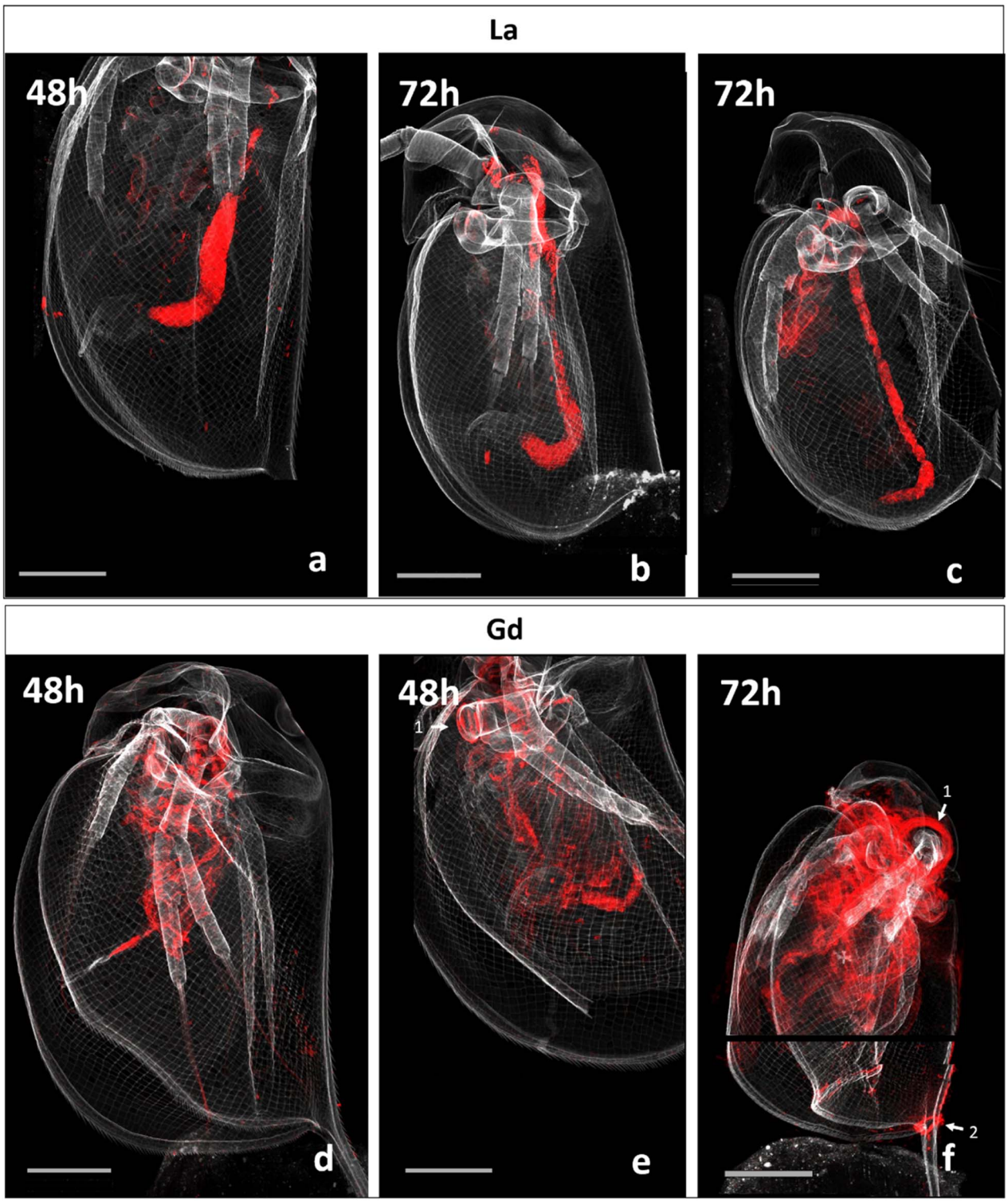


Fig. 2 Lanthanide distribution in juvenile *Daphnia magna*. Grey: calcium, red: lanthanide, scale: 200 μm. Beamline: NANOSCOPIUM. Incident energy of 17.02 keV, pixel size of 1 μm, integration time of 20 ms. (a) Exposure of 15 mg $L^{-1}$ La for 48 h, (b and c) Exposure of 15 mg $L^{-1}$ of La for 72 h. (d and e) Exposure of 15 mg $L^{-1}$ of Gd for 48 h. (f) Exposure of 15 mg $L^{-1}$ of Gd for 72 h. Annotations: (1) anthenna articulation, (2) base of the apical spine.

Zhou *et al.*[11] showed the potential of synchrotron XRF imaging for studying biodistribution of Ln in daphnids. This multi-element analysis offers high spatial resolution 2D mapping and is capable of detecting very low metal concentrations within a complete organism.[13–16] Derived Ln/Ca-ratios show a strong enrichment of Ln in the exposed organism

 

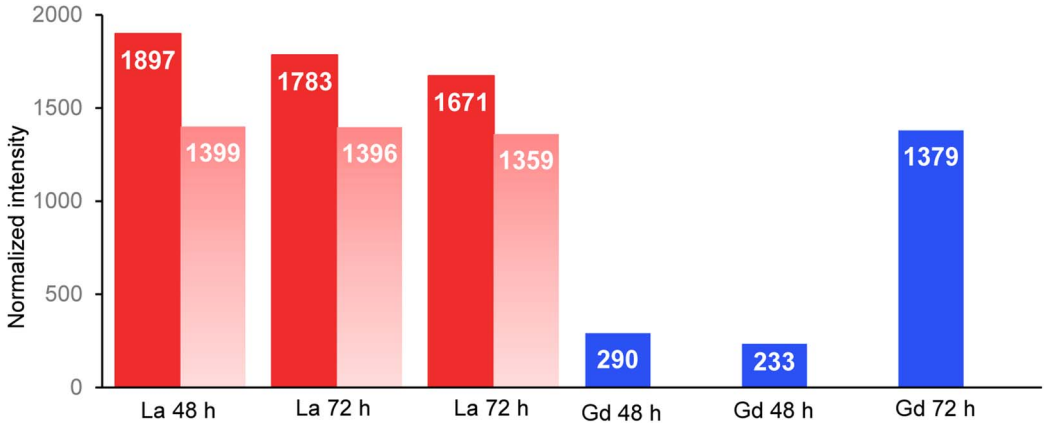


Fig. 3 Normalized intensity of La (red) and Gd (blue) measured in the total organisms and in the intestinal tract (light red) of the organisms. Beamline: NANOSCOPIUM. Incident energy of 17.02 keV.

which exceeds that in the controls by 2 to 3 orders of magnitude (Fig. 5, ESI data S8†). Therefore, the low detection of La and Gd signals in the controls are assumed to be background noise.

While both Ln accumulate in the daphnids, the dorso-ventral profile of Ln intensity of La *versus* Gd exposed daphnid show different distribution patterns (Fig. 7): La seems to be concentrated in the area of the intestinal tract while Gd is widely distributed over the profile. Use of the LUCIA beamline made it possible to map low energy elements (S, P) as indicators of cellular tissue and organs. Co-localisation of Gd with S and P suggests that Gd accumulates in the tissues, such as the gills, maxillary glands and possibly a part of the intestinal tract (ESI data S4†). The calculation of the total normalized intensity of Gd showed a strong increase of one magnitude of its accumulation over time.

The spatial resolution used in this study was as low as 1 to 3 $\mu m^2$, or even down to 0.4 $\mu m^2$ (ESI data S3†). This allowed a thorough visualisation of the metal distribution in the

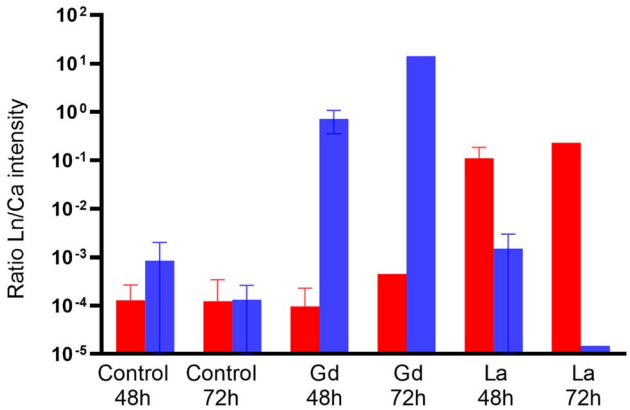


Fig. 5 Ratio between Ln and Ca intensity (logarithmically scaled) for different organisms exposed for 48 and 72 h. Mean and standard deviation. Red: La/Ca, blue: Gd/Ca. Beamline: LUCIA. Incident energy of 7.25 keV.

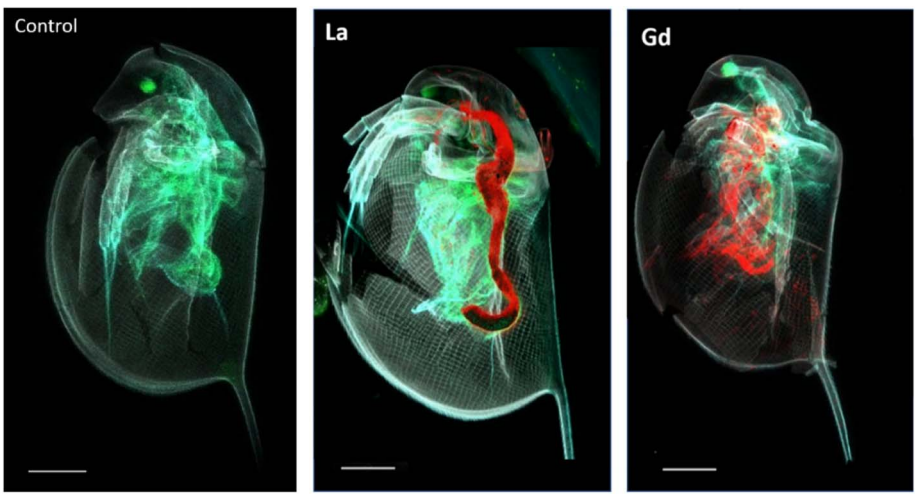


Fig. 4 Calcium (grey), sulfur (green) and phosphorus (blue). La and Gd (red) distribution in juvenile *D. magna* after for 48 h of exposure. Scale: 200 µm. Beamline: LUCIA. Incident energy of 7.25 keV, pixel size of 3 µm and integration time of 80 ms. Control organism (left), La exposure (middle), Gd exposure (right).

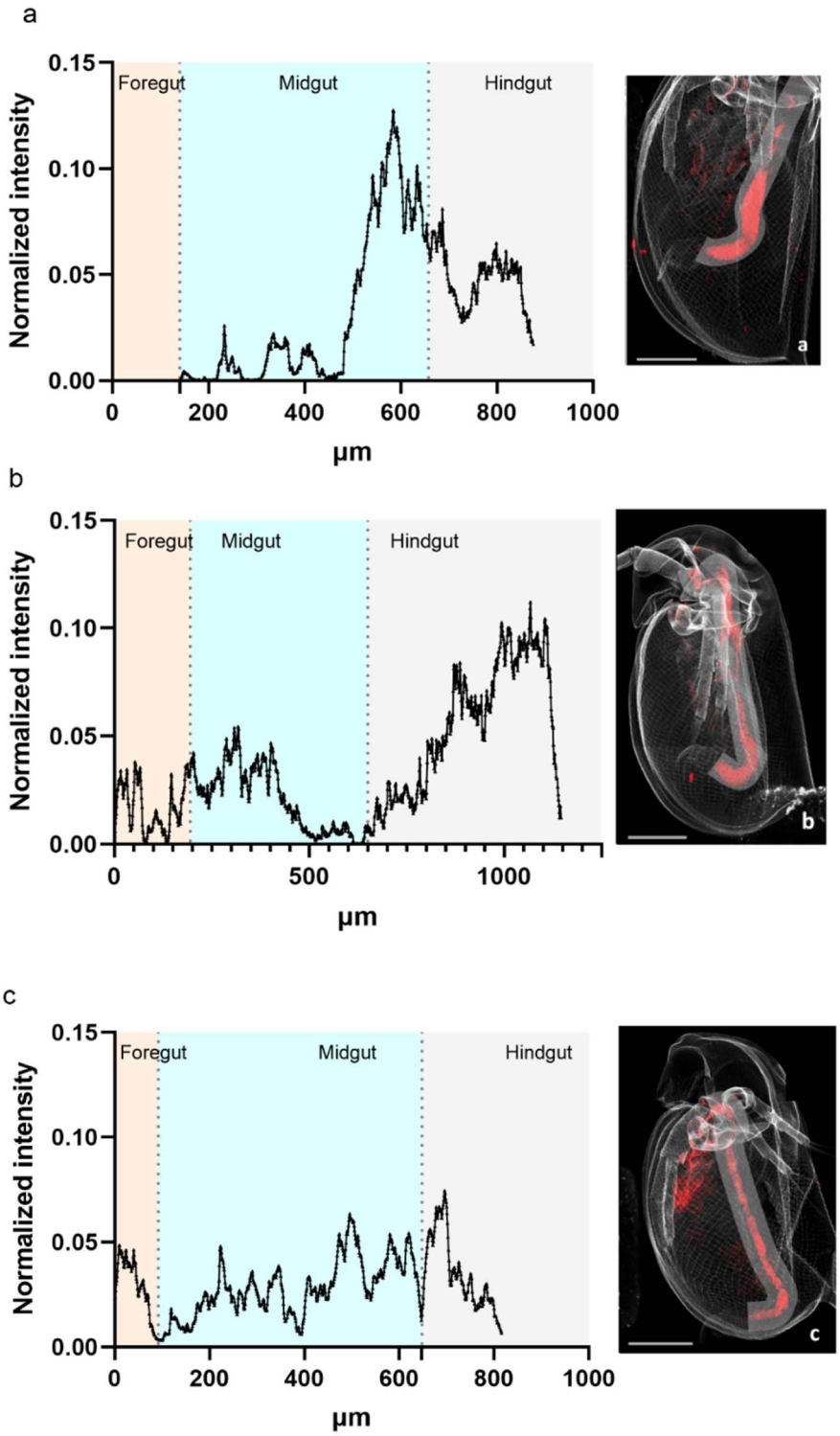


Fig. 6 Variation of La normalized intensity along the intestinal tract of daphnids exposed for 48 h ((a) organism Fig. 2a) and for 72 h ((b) organism Fig. 2b and c, organism Fig. 2c). Line of 90 µm width. Beamline: NANOSCOPIUM. Incident energy of 17.02 keV.

organisms' tissues. Thus, the intestinal tract was clearly defined within the specimens by the ensuing Compton scatter map conducted at high incident energy *i.e.* 17.02 keV. Comparison with the La map verify that accumulation was localized in the gut in an apparently compacted form. It is currently not clear, to what extent La had precipitated in the medium and was taken up by the daphnids in solid form, and what role precipitation in the animal's intestine may play, as the pH increases slightly from the mouth to the anus from pH 6 to pH 7.2.[33,34] Furthermore, it is possible that lower pH in the foregut could enhance

 

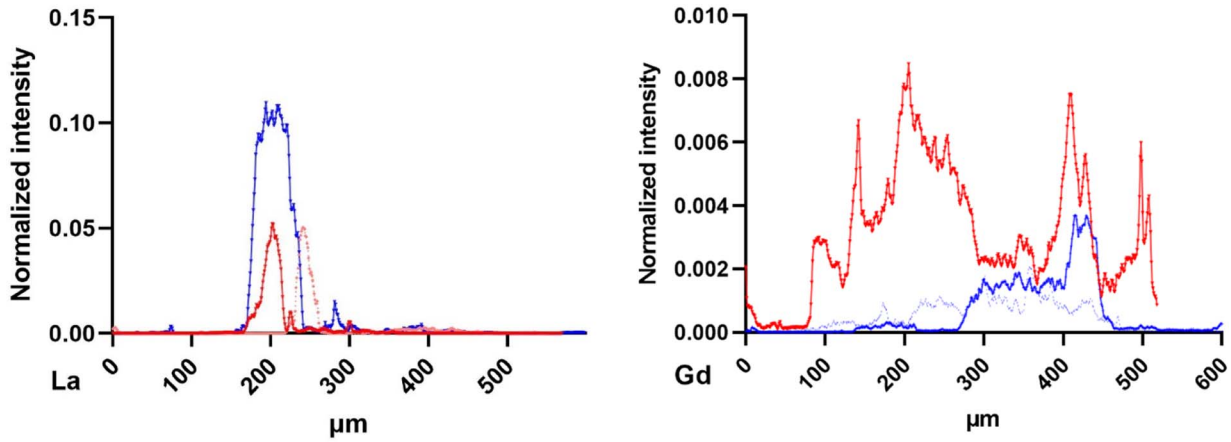


Fig. 7 La (left) and Gd (right) normalized intensity distribution along the dorso-ventral line of 90 µm width from the daphnids of Fig. 2, exposed to 48 h (blue) and 72 h (red). Beamline: NANOSCOPIUM. Incident energy of 17.02 keV.

Table 2 $EC_{50}$ and 95% confidence intervals (in brackets) of La and Gd on the basis of nominal and measured concentrations after 48 h of exposure

| | Nominal $EC_{50}$ (mg $L^{-1}$) | Measured $EC_{50}$ (mg $L^{-1}$) |
|---|---|---|
| Gd | 13.93 (10.92 to 17.38) | 8.22 (7.23 to N.A.) |
| La | >30 | N.A. |

the solubility of metal particles, thereby increasing their bioavailability for the intestinal epithelium. Precipitation in the medium, however, does occur. In the ISO 6341:2013-01 media used here, La and Gd both form complexes and precipitate with carbonate, chlorite, hydroxide or sulphate (ESI data S2†). For the same nominal concentration, the measured concentration of dissolved Gd at the end of exposure tests was significantly higher than for La probably due to lower solubility of $La_2(CO_3)_3$ (Ks: −34.4) compared to $Gd_2(CO_3)_3$ (Ks: −32.2).[35]

Free ions are usually considered to be the major bioavailable and thus effective species[36] (ESI data S2†). In the present case, however, an increased accumulation probably derived from uptake of precipitated solid species in the case of La. Non-selective filter-feeder organisms such as *D. magna* can take up metal precipitates by ingestion. For instance, Heinlaan *et al.*[37] clearly demonstrated a strong accumulation of CuO NPs in *D. magna* gut after 48 h of exposure. In the case of lanthanides, Blinova *et al.*[38] pictured similar accumulation of Ln oxides in the gut of *T. platyurus* while no lethal effect was observed. This conclusion supports the common assumption that the principal lethal toxicity in short-term aquatic toxicity tests results from the water exposure[39] and more precisely from the free metal concentration capable of interacting with the organism's gills.[36]

Therefore, the mobility being affected only by Gd in the present our study, could be explained by the higher concentration of dissolved Gd-species in the media, leading to a more widespread and diffused distribution of Gd in the organisms (ESI data S7†). Once in the tissues, Gd may directly damage the organs or inhibit certain physiological functions when interacting with the daphnid cells. Many studies on freshwater and marine organisms have demonstrated that Gd affects the antioxidant defences of cells and therefore causes oxidant stress.[40] Cunha *et al.*[41] showed in experiments with *Mytilus galloprovincialis* a higher accumulation of La compared to Gd, but a stronger effect of Gd on biochemical pathways during short-term exposure.

The current study showed, that with daphnids, bioaccumulation of La was localized in the intestine and probably in a compacted form that did not compromise the cellular functions noticeably during short-term exposure, while Gd had entered the tissues and significantly lowered mobility of the crustaceans.

This study demonstrates the different uptake and biodistribution patterns of two lanthanides with different toxicity during short term exposure of 2 to 3 days for measured concentrations of 1 to 10 mg $L^{-1}$. These concentrations are well above natural background concentrations (lower ppb range) but are close to concentrations found in stream waters draining from REE mining regions, ranging from 1 to 10 mg $L^{-1}$.[42,43] As daphnids often feed on surfaces, they may take up precipitated REE-containing material. Further work is needed to assess how feeding and longer exposure periods will change toxicity and biodistribution in the crustaceans in order to better estimate whether ecotoxicological concern may arise from increasing Ln emissions to the environment.

## 5. Conclusions

This study provides the first microscale bioaccumulation data for La and Gd in freshwater crustacean. The difference of metal biodistribution observed in *D. magna* resulted in a difference of toxicity which strongly depends on the metal speciation. Under the exposure conditions, La strongly precipitates and the solid particles were easily ingested be the organism, causing a strong bioaccumulation in its intestinal tract. At similar nominal concentration, Gd remained more soluble and triggered

hazardous effect by bioaccumulating in various tissues of the animal. We expect, that it is only in the tissue that Ln can cause oxidative stress and therefore hazardous effects. Even though, relatively high Ln concentrations were used for this study the results provide an important baseline for the toxicokinetics of Ln in the environment.

## Author contributions

Marion Revel was responsible for conducting the bioassays with *Daphnia magna*, preparing the samples for XRF mapping measurements. Delphine Vantelon and Camille Rivard conducted the micro-XRF mapping measurements at Lucia beamline, while Marion Revel, Susanne Heise, and Kadda Medjoubi conducted the nano-XRF mapping measurements at Nanoscopium beamline. The first draft of the paper was written by Marion Revel and Susanne Heise. It was then verified and modified by Delphine Vantelon Camille Rivard, Kadda Medjoubi and Andrew Hursthouse.

## Conflicts of interest

There are no conflicts to declare.

## Acknowledgements

This work was fund by the European Union's Horizon 2020 research and innovation program under the Marie Sklodowska-Curie Grant Agreement No. 857989. The synchrotron nano and micro-XRF beam time was granted by the SOLEIL synchrotron facilities under the project no. 99210292 at LUCIA beamline and project no. 20210472 at NANOSCOPIUM beamline.

## References

1 W. Gwenzi, L. Mangori, C. Danha, N. Chaukura, N. Dunjana and E. Sanganyado, Sources, behaviour, and environmental and human health risks of high-technology rare earth elements as emerging contaminants, *Sci. Total Environ.*, 2018, 636.

2 G. A. MacMillan, J. Chételat, J. P. Heath, R. Mickpegak and M. Amyot, Rare earth elements in freshwater, marine, and terrestrial ecosystems in the eastern Canadian Arctic, *Environ. Sci.: Processes Impacts*, 2017, **19**, 1336–1345.

3 M. J. Barry and B. J. Meehan, The acute and chronic toxicity of lanthanum to Daphnia carinata, *Chemosphere*, 2000, **41**, 1669–1674.

4 H. Herrmann, J. Nolde, S. Berger and S. Heise, Aquatic ecotoxicity of lanthanum – A review and an attempt to derive water and sediment quality criteria, *Ecotoxicol. Environ. Saf.*, 2016, **124**, 213–238.

5 Y. Ma, J. Wang, C. Peng, Y. Ding, X. He, P. Zhang, N. Li, T. Lan, D. Wang, Z. Zhang, F. Sun, H. Liao and Z. Zhang, Toxicity of cerium and thorium on Daphnia magna, *Ecotoxicol. Environ. Saf.*, 2016, **134**, 226–232.

6 E. Galdiero, R. Carotenuto, A. Siciliano, G. Libralato, M. Race, G. Lofrano, M. Fabbricino and M. Guida, Cerium and erbium effects on Daphnia magna generations: A multiple endpoints approach, *Environ. Pollut.*, 2019, **254**, 112985.

7 A. Pałasz and P. Czekaj, Toxicological and cytophysiological aspects of lanthanides action, *Acta Biochim. Pol.*, 2000, **47**, 1107–1114.

8 I. Blinova, A. Lukjanova, M. Muna, H. Vija and A. Kahru, Evaluation of the potential hazard of lanthanides to freshwater microcrustaceans, *Sci. Total Environ.*, 2018, **642**, 1100–1107.

9 U. Borgmann, Y. Couillard, P. Doyle and D. G. Dixon, Toxicity of sixty-three metals and metalloids to Hyalella azteca at two levels of water hardness, *Environ. Toxicol. Chem.*, 2005, **24**, 641–652.

10 C. Blaise, F. Gagné, M. Harwood, B. Quinn and H. Hanana, Ecotoxicity responses of the freshwater cnidarian Hydra attenuata to 11 rare earth elements, *Ecotoxicol. Environ. Saf.*, 2018, **163**, 486–491.

11 T. Zhou, L. Zhang, Y. Wang, Q. Mu and J. Yin, Effects of LaCoO 3 perovskite nanoparticle on Daphnia magna: accumulation, distribution and biomarker responses, *RSC Adv.*, 2019, **9**, 24617–24626.

12 J. Lingott, U. Lindner, L. Telgmann, D. Esteban-Fernández, N. Jakubowski and U. Panne, Gadolinium-uptake by aquatic and terrestrial organisms-distribution determined by laser ablation inductively coupled plasma mass spectrometry, *Environ. Sci.: Processes Impacts*, 2016, **18**, 200–207.

13 B. De Samber, G. Silversmit, R. Evens, K. De Schamphelaere, C. Janssen, B. Masschaele, L. Van Hoorebeke, L. Balcaen, F. Vanhaecke, G. Falkenberg and L. Vincze, Three-dimensional elemental imaging by means of synchrotron radiation micro-XRF: developments and applications in environmental chemistry, *Anal. Bioanal. Chem.*, 2008, **390**, 267–271.

14 B. De Samber, G. Silversmit, K. De Schamphelaere, R. Evens, T. Schoonjans, B. Vekemans, C. Janssen, B. Masschaele, L. Van Hoorebeke, I. Szalóki, F. Vanhaecke, K. Rickers, G. Falkenberg and L. Vincze, Element-to-tissue correlation in biological samples determined by three-dimensional X-ray imaging methods, *J. Anal. At. Spectrom.*, 2010, **25**, 544.

15 B. De Samber, R. Evens, K. De Schamphelaere, G. Silversmit, B. Masschaele, T. Schoonjans, B. Vekemans, C. R. Janssen, L. Van Hoorebeke, I. Szalóki, F. Vanhaecke, G. Falkenberg and L. Vincze, A combination of synchrotron and laboratory X-ray techniques for studying tissue-specific trace level metal distributions in Daphnia magna, *J. Anal. At. Spectrom.*, 2008, **23**, 829.

16 R. Evens, K. A. De Schamphelaere, B. De Samber, G. Silversmit, T. Schoonjans, B. Vekemans, L. Balcaen, F. Vanhaecke, I. Szaloki, K. Rickers, G. Falkenberg, L. Vincze and C. R. Janssen, Waterborne *versus* dietary zinc accumulation and toxicity in Daphnia magna: a synchrotron radiation based X-ray fluorescence imaging approach, *Environ. Sci. Technol.*, 2012, **46**, 1178–1184.

17 OECD,*Test No. 211: Daphnia Magna Reproduction Test*, 2012.

 

18 OECD, *Test No. 202: Daphnia sp. Acute Immobilisation Test*, 2004.
19 D. I. f. Normung, *Water quality - Determination of the Inhibition of the Mobility of Daphnia Magna Straus (Cladocera, Crustacea) - Acute Toxicity Test (ISO 6341:2012); German Version EN ISO 6341:2012*, 2013, DOI: 10.31030/1911255.
20 L. Telgmann, M. Holtkamp, J. Künnemeyer, C. Gelhard, M. Hartmann, A. Klose, M. Sperling and U. Karst, Simple and rapid quantification of gadolinium in urine and blood plasma samples by means of total reflection X-ray fluorescence (TXRF), *Metallomics*, 2011, **3**, 1035–1040.
21 C. Laforsch and R. Tollrian, A new preparation technique of daphnids for Scanning Electron Microscopy using hexamethyldisilazane, *Arch. Hydrobiol.*, 2000, 587–596.
22 A. Somogyi, K. Medjoubi, G. Baranton, V. Le Roux, M. Ribbens, F. Polack, P. Philippot and J. P. Samama, Optical design and multi-length-scale scanning spectro-microscopy possibilities at the Nanoscopium beamline of Synchrotron Soleil, *J. Synchrotron Radiat.*, 2015, **22**, 1118–1129.
23 A. M. Flank, G. Cauchon, P. Lagarde, S. Bac, M. Janousch, R. Wetter, J. M. Dubuisson, M. Idir, F. Langlois, T. Moreno and D. Vantelon, LUCIA, a microfocus soft XAS beamline, *Nucl. Instrum. Methods Phys. Res., Sect. B*, 2006, **246**, 269–274.
24 D. Vantelon, N. Trcera, D. Roy, T. Moreno, D. Mailly, S. Guilet, E. Metchalkov, F. Delmotte, B. Lassalle, P. Lagarde and A.-M. Flank, The LUCIA beamline at SOLEIL, *J. Synchrotron Radiat.*, 2016, **23**, 635–640.
25 D. L. Howard, M. D. de Jonge, N. Afshar, C. G. Ryan, R. Kirkham, J. Reinhardt, C. M. Kewish, J. McKinlay, A. Walsh, J. Divitcos, N. Basten, L. Adamson, T. Fiala, L. Sammut and D. J. Paterson, The XFM beamline at the Australian Synchrotron, *J. Synchrotron Radiat.*, 2020, **27**, 1447–1458.
26 K. Medjoubi, N. Leclercq, F. Langlois, A. Buteau, S. Lé, S. Poirier, P. Mercere, M. C. Sforna, C. M. Kewish and A. Somogyi, Development of fast, simultaneous and multi-technique scanning hard X-ray microscopy at Synchrotron Soleil, *J. Synchrotron Radiat.*, 2013, **20**, 293–299.
27 C. A. Schneider, W. S. Rasband and K. W. Eliceiri, NIH Image to ImageJ: 25 years of image analysis, *Nat. Methods*, 2012, **9**, 671–675.
28 V. A. Solé, E. Papillon, M. Cotte, P. Walter and J. Susini, A multiplatform code for the analysis of energy-dispersive X-ray fluorescence spectra, *Spectrochim. Acta, Part B*, 2007, **62**, 63–68.
29 P. Tai, Q. Zhao, D. Su, P. Li and F. Stagnitti, Biological toxicity of lanthanide elements on algae, *Chemosphere*, 2010, **80**, 1031–1035.
30 L. R. Bergsten-Torralba, D. P. Magalhães, E. C. Giese, C. R. S. Nascimento, J. V. A. Pinho and D. F. Buss, Toxicity of three rare earth elements, and their combinations to algae, microcrustaceans, and fungi, *Ecotoxicol. Environ. Saf.*, 2020, **201**, 110795.
31 V. González, D. A. L. Vignati, M.-N. Pons, E. Montarges-Pelletier, C. Bojic and L. Giamberini, Lanthanide ecotoxicity: First attempt to measure environmental risk for aquatic organisms, *Environ. Pollut.*, 2015, **199**, 139–147.
32 K. Chojnacka and M. Mikulewicz, in *Encyclopedia of Toxicology*, ed. P. Wexler, Academic Press, Oxford, 3rd edn, 2014, pp. 456–460, DOI: 10.1016/B978-0-12-386454-3.01039-3.
33 A. Davis, F. Nasser, J. R. Lead and Z. Shi, Development and application of a ratiometric nanosensor for measuring pH inside the gastrointestinal tract of zooplankton, *Environ. Sci.: Nano*, 2020, **7**, 1652–1660.
34 D. Ebert, *Ecology, Epidemiology, and Evolution of Parasitism in Daphnia*, National Library of Medicine, 2005.
35 R. Smith, A. Martell and R. Motekaitis, *NIST standard reference database 46, NIST critically selected stability constants of metal complexes database Ver*, 2004, 2.
36 D. M. Di Toro, H. E. Allen, H. L. Bergman, J. S. Meyer, P. R. Paquin and R. C. Santore, Biotic ligand model of the acute toxicity of metals. 1. Technical Basis, *Environ. Toxicol. Chem.*, 2001, **20**, 2383–2396.
37 M. Heinlaan, A. Kahru, K. Kasemets, B. Arbeille, G. Prensier and H. C. Dubourguier, Changes in the Daphnia magna midgut upon ingestion of copper oxide nanoparticles: a transmission electron microscopy study, *Water Res.*, 2011, **45**, 179–190.
38 I. Blinova, M. Muna, M. Heinlaan, A. Lukjanova and A. Kahru, Potential hazard of lanthanides and lanthanide-based nanoparticles to aquatic ecosystems: data gaps, challenges and future research needs derived from bibliometric analysis, *Nanomaterials*, 2020, **10**, 328.
39 S. E. Hook and N. S. Fisher, Sublethal effects of silver in zooplankton: importance of exposure pathways and implications for toxicity testing, *Environ. Toxicol. Chem.*, 2001, **20**, 568–574.
40 G. Trapasso, S. Chiesa, R. Freitas and E. Pereira, What do we know about the ecotoxicological implications of the rare earth element gadolinium in aquatic ecosystems?, *Sci. Total Environ.*, 2021, **781**, 146273.
41 M. Cunha, P. Louro, M. Silva, A. M. V. M. Soares, E. Pereira and R. Freitas, Biochemical alterations caused by lanthanum and gadolinium in Mytilus galloprovincialis after exposure and recovery periods, *Environ. Pollut.*, 2022, **307**, 119387.
42 T. Liang, K. Li and L. Wang, State of rare earth elements in different environmental components in mining areas of China, *Environ. Monit. Assess.*, 2014, **186**, 1499–1513.
43 W.-S. Liu, M.-N. Guo, C. Liu, M. Yuan, X.-T. Chen, H. Huot, C.-M. Zhao, Y.-T. Tang, J. L. Morel and R.-L. Qiu, Water, sediment and agricultural soil contamination from an ion-adsorption rare earth mining area, *Chemosphere*, 2019, **216**, 75–83.